Macromolecules

pubs.acs.org/Macromolecules Article

How Does the Character of Glassy-Polymeric Cavitation Depend on Entanglement Density and the Local Poisson Ratio?

Kai Nan, Pedro Abritta, and Robert S. Hoy*

Cite This: *Macromolecules* 2021, 54, 7347−7353 Read Online

ACCESS | Metrics & More | Article Recommendations

ABSTRACT: Using molecular dynamics simulations of two generic glassy polymers, we distinguish factors promoting cavitation that is followed by unrestrained void growth and coalescence (i.e. by crazing and brittle fracture) from "ductile" cavitation that does not lead to massive void growth. Strain-controlled deformation in a wide range of wide Poisson ratios ν reveals several features not apparent from the uniaxial-deformation or uniaxial-stress protocols employed by the vast majority of previous studies. In particular, for $0.125 \lesssim \nu \lesssim 0.45$, semiflexible, tightly entangled chains have a significantly lower void volume fraction (but far more voids) at the same strain and volumetric expansion ratio than their flexible, loosely entangled counterparts. Voids in loosely entangled glasses coalesce more often and grow faster, whereas voids in tightly (but not loosely) entangled glasses continue to nucleate well into the strain-hardening regime.

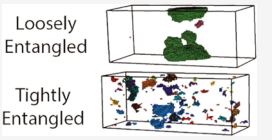

1. INTRODUCTION

Predicting the toughness of glassy-polymeric samples from their microscopic physical properties is a longstanding challenge. Even for a given polymer chemistry and chain length distribution, the sample's thermomechanical history, the ambient conditions under which it is deformed, and the deformation protocol to which it is subjected are often the factors that determine whether it will be brittle or ductile. A key aspect of this problem is the interplay between cavitation and crazing. Cavitation often leads to massive void growth and coalescence, i.e., to crazing and eventual brittle fracture.[1,2] On the other hand, cavitation that does not lead to crazing is also common and can be an effective means of energy dissipation during ductile deformation.[3]

Determining which type of cavitation will occur for a given sample and deformation protocol, however, is quite difficult in general. Although macroscopic criteria for craze initiation such as the triaxiality of tensile stress[2] and the fact that the crossover from shear yielding to cavitation is demarcated by a change in the slope α and offset τ_0 in the pressure-modified von Mises criterion $\tau_y = \tau_0 + \alpha P$ are well established,[4,5] much remains unknown about which factors control whether nucleated cavities will grow into stable crazes. Indeed, determining which microscopic features control the relationship between cavitation and fracture remains an active field of study for a wide variety of soft-matter systems.[6]

Such features are neither straightforward to characterize experimentally nor readily treated by either continuum or microscopic analytic theories, but particle-based simulations can offer many insights. Most previous simulations of glassy-polymeric cavitation and crazing have employed a single deformation protocol: uniaxial-strain extension where the sample's transverse dimensions are held constant.[7−16] To elucidate the role played by the large volumetric expansion inherent to this protocol, results from these simulations have often been compared to results for other protocols such as uniaxial-stress compression, simple shear, or constant-volume pure shear.[17−22]

The local deformation of a real glassy-polymeric sample, however, is by no means limited to these simple modes. In particular, representative volume elements (RVEs) within a sample under tensile stress may undergo deformation ranging from nearly uniaxial extension in a craze ahead of a crack tip to nearly constant-volume pure shear during neck formation. Deformation modes lying between these idealized limits are common, particularly, in samples subjected to triaxial loads. Such modes may play a key role in determining such samples' ultimate mechanical response but (apart from uniaxial-stress extension[23−26]) have rarely been studied in any detail in the postyield regime.

In this paper, we fill this gap in the literature by extending the study of model polymer glasses at a constant Poisson ratio ν. Our deformation protocol continuously interpolates between the abovementioned idealized limits as ν increases from 0 to 1/2. To avoid complications arising from temperature's strong influence on the shearing-versus-crazing competition, we study systems in the $T \to 0$ limit, which maximally favors crazing and brittle fracture.[27] We contrast the results for two very different glasses: one flexible-chain, loosely entangled glass with high packing efficiency and homogeneity

Received: May 25, 2021
Revised: July 8, 2021
Published: August 11, 2021

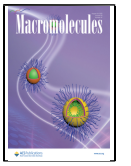

https://doi.org/10.1021/acs.macromol.1c01128
Macromolecules 2021, 54, 7347−7353

and one semiflexible-chain, tightly entangled glass with less-efficient, more heterogeneous packing. The former is intended to be representative of ductile glasses which often craze (e.g. PMMA), while the latter is intended to be representative of glasses which usually shear-band (e.g. PC).[27−30]

We find that for a wide range of ν and hence for a wide range of triaxial-stress histories, the overall void volume fraction f_v remains significantly smaller in the tightly entangled glass than its loosely entangled counterpart when systems are compared at the same axial strain ϵ and volumetric expansion ratio $\mathcal{V}(\varepsilon, \nu) \equiv V(\varepsilon, \nu)/V_0 = \exp[(1 - 2\nu)\varepsilon]$, despite the fact that many more voids nucleate in the tightly entangled glass during cavitation. Voids in the loosely entangled glass coalesce far more often and grow faster, while voids in the tightly (but not the loosely) entangled glass continue to nucleate at a significant rate well into the strain-hardening regime, providing an additional mechanism for energy dissipation. Thus, our loosely (tightly) entangled glasses roughly correspond to the cases where cavitation does (does not) quickly lead to brittle fracture. Below, we describe these results in detail and then place them in context with recent simulations and experiments.

2. MODEL AND METHODS

We study the ν-dependence of cavitation and void growth using molecular dynamics simulations of a bead-spring model[31,32] which has been shown to capture many features of glassy-polymeric mechanical response.[33] All monomers have mass m and interact via the truncated and shifted Lennard-Jones potential

$$U_{LJ}(r) = 4\varepsilon\left[\left(\frac{a}{r}\right)^{12} - \left(\frac{a}{r}\right)^{6} - \left(\frac{a}{r_c}\right)^{12} + \left(\frac{a}{r_c}\right)^{6}\right] \quad (1)$$

where ε is the intermonomer binding energy, a is monomer diameter, and $r_c = 2^{7/6}a$ is the cutoff radius. The Lennard-Jones time unit is $\tau = \sqrt{ma^2/\varepsilon}$, and the MD timestep employed in this study is $\delta t = \tau/200$.

Covalent bonds are modeled using a quartic potential suitable for studies of fracture[32]

$$U_{qu}(l) = k_q(l - R_b)^3(l - R_b - B_2) \quad (2)$$

Bonds break when their length (l) exceeds $R_b = 1.3a$. B_2 is selected by matching $U_{qu}(l)$ to the first zero and the minimum of U_{FENE}, which sets $B_2 = -0.4668a$. As in many previous studies of bead-spring glasses' fracture mechanics,[34] the ratio of the forces at which covalent and van der Waals bonds break is set to 100 by setting $k_q = 9640\varepsilon/a^4$.

Angular interactions between three consecutive beads along chain backbones are modeled using the standard potential $U_b(\theta) = \kappa(1 - \cos(\theta))$, where θ_i is the angle between consecutive bond vectors $\vec{b}_i$ and $\vec{b}_{i+1}$; note that θ is zero and U_b is minimized for straight trimers. We consider two chain stiffnesses here: flexible ($\kappa = 0$) and semiflexible ($\kappa = 2\varepsilon$). The latter κ produces tight entanglement[35] which leads to dramatic, "Langevin" strain hardening and more-violent plastic deformation and fracture.[22,36,37]

All molecular dynamics simulations are performed using LAMMPS.[38] Systems are composed of $N_{ch} = 500$ linear chains of $N = 600$ monomers. Periodic boundary conditions are applied along all three directions. Systems were prepared by very slowly cooling well-equilibrated melts to $T = 0$ as described in ref 22. This protocol produces fairly well-aged glasses that can exhibit significant strain softening. The entanglement lengths in the final $T = 0$ states are respectively $N_e = 70$ and $N_e = 15$ for $\kappa = 0$ and $\kappa = 2\varepsilon$.

Following the cooling runs, we extend systems along their z-axes at a constant Poisson ratio

$$\nu = -\frac{d\varepsilon_{trans}}{d\varepsilon_{axial}} = -\frac{d\varepsilon_{xx}}{d\varepsilon_{zz}} = -\frac{d\varepsilon_{yy}}{d\varepsilon_{zz}} \quad (3)$$

where $\bar{\epsilon}$ is their true strain tensor. We examine the entire range of Poisson ratios ($0 \le \nu \le 1/2$) that is likely to be sampled by RVEs of extensionally deformed samples; recall that $\nu = 0$ and $\nu = 1/2$ correspond to the well-studied uniaxial extension and constant-volume extension limits.[5,9,17] The applied (true) strain rate, $\dot{\epsilon} \equiv \dot{\epsilon}_{zz} = 10^{-5}/\tau$, is small enough to be near the quasistatic limit for the very low temperature we employ.[39] We deform systems at this rate until they have reached $\epsilon = \epsilon_{term} = 0.7$, which corresponds to a final extension ratio $\lambda_{term} = \exp(0.7) \simeq 2$. This strain is sufficiently large to probe cavitation and craze initiation (or the lack thereof), which are our primary interest. We found that bond scission was negligible for all runs.

We monitor void nucleation, growth, and coalescence by dividing simulation cells into $N_c(\epsilon) = n_x(\epsilon) \times n_y(\epsilon) \times n_z(\epsilon)$ subcells of side lengths $l_x(\epsilon) = L_x(\epsilon)/\text{floor}[L_x(\epsilon)/a]$, $l_y(\epsilon) = L_y(\epsilon)/\text{floor}[L_y(\epsilon)/a]$, and $l_z(\epsilon) = L_z(\epsilon)/\text{floor}[L_z(\epsilon)/a]$. Here $L_z(\epsilon) = L_0\ \exp(\epsilon)$, $L_x(\epsilon) = L_y(\epsilon) = L_0\ \exp(-\nu\epsilon)$, and $L_0 \simeq 65a$ are the initial (κ-dependent) simulation cell side lengths, and floor[x] rounds x downward to the nearest integer, e.g., floor[8.7] = 8. The number of void cells $N_{vc}(\epsilon)$ is the number of subcells that contain no monomer cores, where a core is defined as a sphere of diameter a centered on the given monomer's position, and the void volume fraction is $f_v(\epsilon) = N_{vc}(\epsilon)/N_c(\epsilon)$. We divide the void cells into $N_{dv}(\epsilon)$ distinct (topologically disconnected) voids using connected component analysis[40] and calculate the void size statistics, focusing on $f_{mv}(\epsilon)$, the volume fraction occupied by the largest void.

3. RESULTS

We begin by discussing systems' macroscopic mechanical response. Figure 1 shows the axial stress σ_{zz}, the pressure P, and the normal stress difference $\Delta = \sigma_{zz} - (\sigma_{xx} + \sigma_{yy})/2$, for flexible chains, for a wide range of ν. All results for $\nu = 0$ are similar to those reported in previous simulation studies of crazing which used uniaxial-strain deformation:[7−16] an elastic regime, followed by very sharp cavitation-induced yielding and massive strain softening, which is followed by stable craze drawing at nearly constant stress. All results for $\nu = 0.5$ are comparable to those reported in previous studies of uniaxial-stress extension:[23−26] the much greater strain softening and much lower σ_{zz} for $\epsilon \gtrsim 0.1$ are caused by the positive pressure produced by the constant-volume constraint [panel (b)]. Here our main focus is on intermediate ν.

Panels (a−b) show similar trends for all $\nu \le 0.375$. Simultaneous sharp drops in σ_{zz} and increases in P indicate cavitation-induced yielding,[4,5] eventually followed by stable craze drawing. As expected, the yield strains increase and the yield stresses decrease monotonically with increasing ν. The cavitation pressures P_{cav} (i.e. the minima in P) increase monotonically with increasing ν. Intriguingly, however, systems' densities at cavitation (Table 1) remain nearly constant, suggesting that the heights of the lowest energy barriers to cavitation in actively deformed polymer glasses depend primarily on $\mathcal{V}$ and only secondarily on the anisotropy of $\bar{\epsilon}$ and $\bar{\sigma}$.

For $\nu \gtrsim 0.4$, the $\sigma_{zz}(\epsilon)$ curves show two maxima—gradual yielding at $\epsilon = \epsilon_y(\nu)$ followed by sharper drops at $\epsilon = \epsilon_{cav}(\nu)$. The reason these curves are qualitatively different from their $\nu \le 0.375$ counterparts is very simple: the "natural" Poisson ratio (obtained by additional pressure-controlled simulations that imposed zero transverse stress rather than fixing ν) ν_{nat} is 0.40. All the curves for $\nu > \nu_{nat}$ are consistent with initial shear yielding followed by eventual crazing, which often occurs when

https://doi.org/10.1021/acs.macromol.1c01128
Macromolecules 2021, 54, 7347−7353

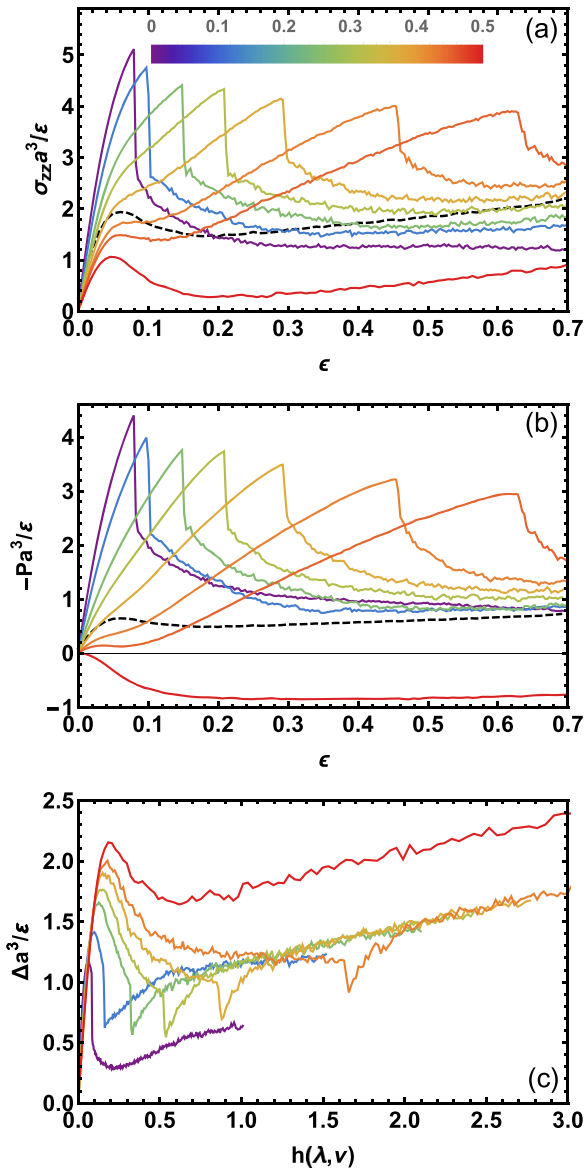

Figure 1. Axial true stress $\sigma_{zz}(\epsilon)$ [panel (a)], pressure $P(\epsilon)$ [panel (b)], and normal stress difference $\Delta[h(\lambda, \nu)]$ [panel (c)] for flexible ($\kappa = 0$) chains, for $\nu = 0$, 0.125, 0.25, 0.3125, 0.375, 0.425, 0.45, and 0.5. For clarity, results for $\nu = 0.45$ are omitted from panel (c). The bar legend indicates ν, and dashed black curves in panels (a,b) show results for uniaxial-stress runs with $\sigma_{trans} = 0$.

samples extend well beyond necking before fracturing.[28] None of this is surprising in and of itself, but shear yielding followed by (sometimes much later) crazing has rarely been studied in simulations of bulk polymer glasses, and we will show below that it leads to a void-growth phenomenology that is significantly different from its $\nu < \nu_{nat}$ counterpart.

Sharp insights into these systems' mechanical response can be obtained by analyzing the systems' $\Delta(\lambda)$, where $\lambda = \ln(\epsilon) = L_z/L_0$ is the axial stretch. Ductile polymers typically exhibit at least some strain hardening, an increase in true stress that occurs in the postyield regime. Gaussian strain hardening, i.e., $\Delta(\lambda) \simeq \sigma_{flow} + G_R h(\lambda, \nu)$, where G_R is the polymer's strain-hardening modulus, $h(\lambda, \nu) = g(\lambda, \nu) - g(1, \nu)$, and $g(\lambda, \nu) \equiv \lambda^{2\nu+1} - 2\nu\lambda^{-1}$, is observed in the postyield regime for most ductile polymer glasses.[36,41] For $\nu = 0$ and $\nu = 1/2$, $g(\lambda, \nu)$ reduces to the familiar forms λ and $\lambda^2 - 1/\lambda$, which are often used to characterize Δ in studies of uniaxial-strain and uniaxial-stress extension.

Table 1. Cavitation Strains, Pressures, and Densities for Flexible and Semiflexible Chains[a]

	$\kappa = 0$			$\kappa = 2\epsilon$		
ν	ϵ_{cav}	$-P_{cav}$	ρ_{cav}	ϵ_{cav}	$-P_{cav}$	ρ_{cav}
0	0.078	4.59	1.009	0.069	3.81	0.996
0.125	0.097	4.00	1.015	0.090	3.57	0.999
0.25	0.147	3.82	1.014	0.145	3.42	0.995
0.3125	0.207	3.79	1.010	0.192	3.29	0.996
0.375	0.291	3.52	1.015	0.284	3.03	0.998
0.425	0.453	3.32	1.020	0.438	2.65	1.004
0.45	0.627	2.95	1.025	0.570	2.45	1.013

[a]Pressures are given in units of ϵa^{-3} and densities in units of a^{-3}. For reference, the initial (unstrained) densities for $\kappa = 0$ and $\kappa = 2\epsilon$ are respectively $\rho_0 = 1.092$ and $\rho_0 = 1.073$. Note that we define ϵ_{cav} as the strain at which pressure is minimized even when the minimum is not sharp.

Panel (c) shows $\Delta[h(\lambda, \nu)]$ for all $0 \le \nu \le 1/2$. Evidently, all systems share a common elastic response at small strains before yielding in the order of increasing ν. Beyond yield, Δ depends strongly on ν, in ways that were not apparent from examining σ_{zz} and P. For $0.125 \le \nu \le 0.45$, all systems show a sharp minimum in Δ at $\epsilon = \epsilon_{cav}$, followed by sharp linear increases, followed by more gradual linear increases corresponding to Gaussian strain hardening. The transition between the sharp and gradual regimes occurs when Δ has reached the common $\Delta = \sigma_{flow} + G_R h(\lambda, \nu)$ curve. In the sharp-increase regime, the systems' axial stress σ_{zz} slowly decreases, whereas their transverse stress $\sigma_{trans} = (\sigma_{xx} + \sigma_{yy})/2$ more rapidly decreases; a linear increase in Δ occurs because $d\sigma_{zz}/dh - d\sigma_{trans}/dh$ is roughly constant.

In contrast, for $\nu = 0$, $d\sigma_{zz}/dh - \sigma_{trans}/dh$ is initially negative but then immediately begins increasing, and the transition between the sharp and gradual linear-increase regimes is obscured; thus it was missed by previous simulation studies of crazing that only employed $\nu = 0$ deformation.[7−16] At larger strains, the Δ values for $\nu = 0$ and $\nu = 1/2$ fail to collapse onto the common strain-hardening response because $\sigma_{trans}(\epsilon, \nu)$ increases much faster than $\sigma_{zz}(\epsilon, \nu)$ as ν decreases toward 0 and decreases much faster than $\sigma_{zz}(\epsilon, \nu)$ as ν increases toward 1/2. Our main purpose in discussing these features is to demonstrate that systems deformed via our constant-ν protocol with $0 < \nu < 1/2$ have a common mechanical response which is distinct from those for the rather artificial $\nu = 0$ and $\nu = 1/2$ cases.[42]

Figure 2 shows the same quantities as Figure 1 but for semiflexible ($\kappa = 2\epsilon$) chains. In all panels, results are qualitatively different than those discussed above. The maxima in $\sigma_{zz}(\epsilon)$ and $|P(\epsilon)|$ are considerably less sharp even for $\nu = 0$, and both weaken and broaden rapidly with increasing ν. The deep, sharp minima in Δ are replaced by shallower, broader minima, especially for $\nu \gtrsim 0.125$. The supralinear-in-h (Langevin) hardening exhibited by these systems is typical of tightly entangled polymer glasses:[36] again, all systems with $0 < \nu < 0.5$ exhibit a common response. Nothing in any of the stress−strain curves for $\nu \gtrsim 0.35$ indicates cavitation of the type experienced by flexible chains deformed at the same ν.

Overall, the contrasting behaviors of loosely and tightly entangled glasses shown in Figures 1 and 2 all suggest that the former undergo cavitation followed by crazing for deformation

https://doi.org/10.1021/acs.macromol.1c01128
Macromolecules 2021, 54, 7347−7353

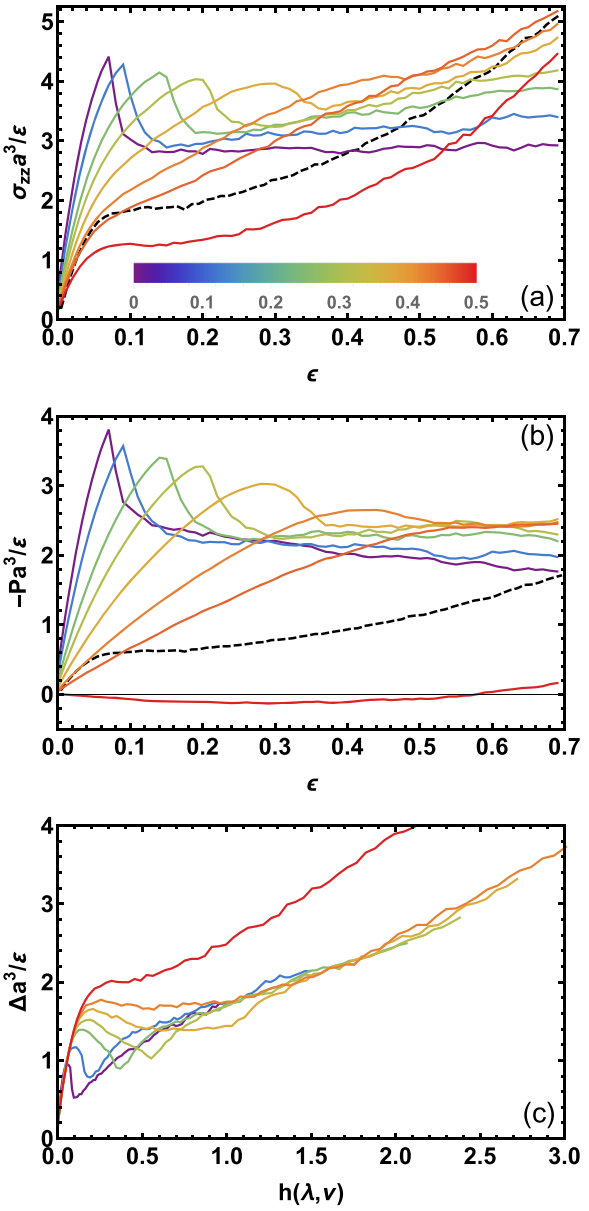

Figure 2. Axial true stress $\sigma_{zz}(\epsilon)$ [panel (a)], pressure $P(\epsilon)$ [panel (b)], and normal stress difference $\Delta[h(\lambda, \nu)]$ [panel (c)] for semiflexible ($\kappa = 2\epsilon$) chains, for ν = 0, 0.125, 0.25, 0.3125, 0.375, 0.425, 0.45, and 0.5. The bar legend indicates ν, and dashed black curves in panels (a,b) show results for uniaxial-stress runs with σ_{trans} = 0.

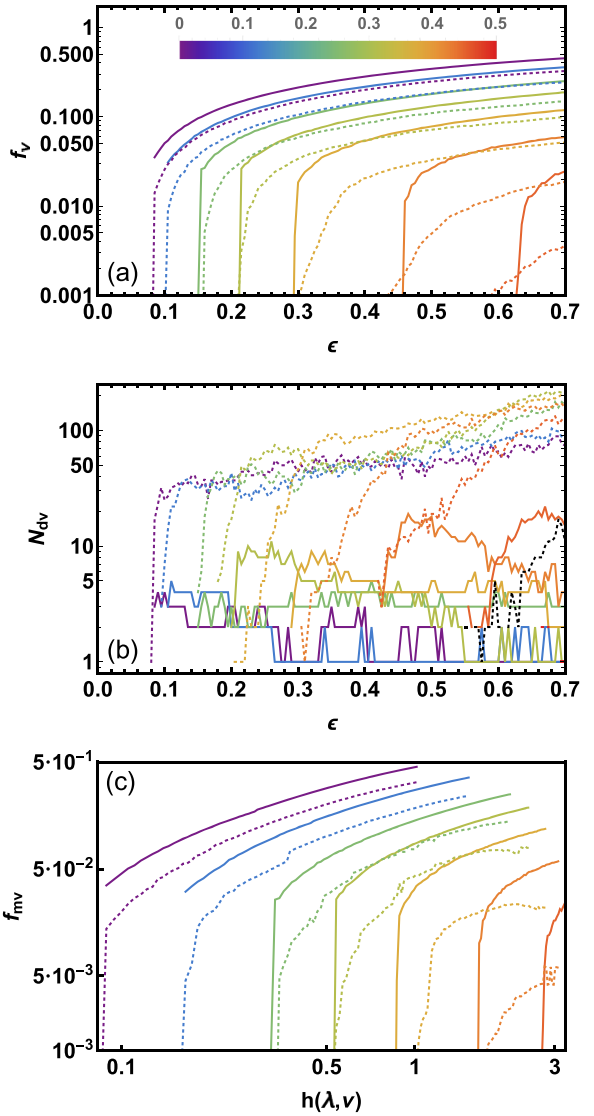

Figure 3. Void volume fraction f_v [panel (a)], number of distinct voids N_{dv} [panel (b)], and volume fraction occupied by the largest void f_{mv} [panel (c)] for flexible $\kappa = 0$ (solid curves) and semiflexible $\kappa = 2\epsilon$ (dashed curves) chains, for ν = 0, 0.125, 0.25, 0.3125, 0.375, 0.425, and 0.45; the bar legend indicates ν; all quantities are negligible for the ν = 0.5 and σ_{trans} = 0 runs.

protocols spanning the range $0.125 \lesssim \nu \lesssim 0.45$, while the latter does not. All results are consistent with the well-established idea that tighter entanglement favors shear yielding over crazing.[1,2,28,29] However, since $\mathcal{V}(\nu, \varepsilon)$ is the same for both systems, the $\kappa = 2\epsilon$ glasses cannot simply be shear-yielding in the same manner as they would in a uniaxial-stress experiment. Cavitation must be occurring, but of a sort that does not have a clear signature in their stress−strain curves. To solve this puzzle, we examine in detail how voids in both glasses nucleate, grow, and merge during deformation.

Figure 3 shows results for the three void metrics discussed in Section 2. Panel (a) shows that for all ν and ϵ, the void volume fraction $f_v(\epsilon)$ is substantially lower in the tightly entangled glass. For ν = 0, the differences are relatively small—for example, flexible chains have a terminal $f_v(0.7) = 0.451$ while semiflexible chains' have a terminal $f_v(0.7) = 0.325$—and are clearly quantitative rather than qualitative. They may arise primarily from the $\kappa = 0$ glasses' larger craze extension ratios and interfibril spacings.[9] As ν increases, however, the differences become much more dramatic. The volumes of the initially nucleated cavities (i.e. the size of the initial jumps in f_v) for $\kappa = 2\epsilon$ glasses progressively shrink relative to those for $\kappa = 0$, and subsequent void growth becomes progressively slower. For $\nu \gtrsim 0.4$, the void volume fractions in the common strain-hardening regimes [Figures 1c and 2c] are almost one order of magnitude lower for $\kappa = 2\epsilon$.

Other metrics show that the differences in these systems' cavitation and void-growth phenomenology are even greater than those suggested by the differences in f_v. Panel (b) shows that for all ν, the number of topologically distinct voids N_{dv} is at least an order of magnitude larger for semiflexible chains. Another qualitative difference is that for flexible chains with all

https://doi.org/10.1021/acs.macromol.1c01128
Macromolecules 2021, 54, 7347−7353

$\nu < \nu_{nat}$, the voids that nucleate tend to merge; N_{dv} stays flat or decreases as strain increases. Comparable results (for $\nu = 0$) were recently reported in ref 16; such void coalescence is probably an essential ingredient for brittle fracture. For semiflexible chains, however, N_{dv} increases monotonically with strain for all ν, indicating not only that void coalescence is minimal in these systems but also that new voids continue to be nucleated during strain hardening. As a side note, the growth in N_{dv} at moderate strains in flexible chains with $\nu \gtrsim \nu_{nat}$ corresponds to the fact that barriers to void nucleation are lower in systems which have just shear-yielded or (more generally) been mechanically rejuvenated.[43]

Panel (c) shows how the volume fractions f_{mv} occupied by the largest voids in the systems increase with strain. The slope $\gamma \equiv d[\ln(f_{mv})]/d[\ln(h)]$ indicates the power law with which f_{mv} grows with h: $\gamma < 1$ ($\gamma > 1$) indicates sublinear (supralinear) growth. Results for flexible chains indicate void growth that is weakly stabilized by strain hardening; as their $\Delta[h(\lambda, \nu)]$ increases linearly with h [Figure 1c], their γ gradually decreases. Again, results for $\kappa = 2\epsilon$ chains are qualitatively different, especially for $\nu > 0.125$. Although these systems can form medium-size voids ($\sim 1/3 - 1/2$ the size of those found in their flexible-chain counterparts), the growth of these voids is clearly stabilized by strain hardening to a much greater degree. In particular, the much faster decrease in their γ is presumably directly associated with the faster increase in their $d\Delta/dh$ [Figure 1c]. While both glasses' γ remains below 1 for all ν and all $\epsilon_{cav} < \epsilon \leq \epsilon_{term}$, we expect that their γ will increase rapidly at larger strains; supralinear void growth has very recently been identified[44,45] as an immediate precursor to brittle fracture.

Figure 4 illustrates the essential differences between our loosely and tightly entangled glasses. The snapshots show terminal configurations for $\nu = 0.375$; the fractional volumetric expansion for both systems is $\mathcal{V}(0.7, 375) - 1 = 19\%$. The

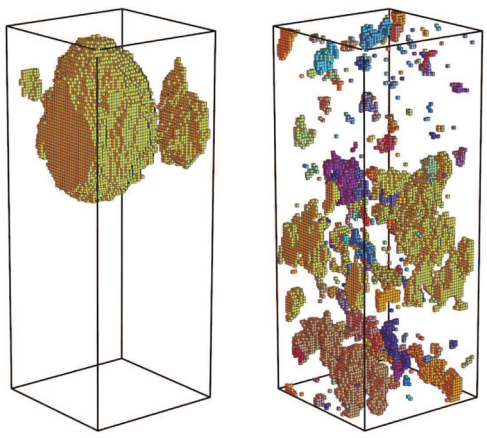

Figure 4. Voids in $\kappa = 0$ (left) and $\kappa = 2\epsilon$ (right) glasses deformed at $\nu = 0.375$, at the terminal strain $\epsilon_{term} = 0.7$. Different colors are assigned to topologically distinct voids. For both systems, the gold-colored void is the largest. Note that the $\mathcal{V}$ we have considered and f_v we have reported in this paper for $\nu \leq 0.45$ and large strains are substantially larger than those observed in experiments where f_v is obtained by averaging over a large volume. In such experiments, samples' $\mathcal{V}$ and f_v typically remain well below 10% and 0.1%, respectively.[44,45] Our simulation cells, however, are RVEs corresponding to the internal regions of an experimental sample where strain localizes and hence dilatative deformation is much greater.[9]

final void volume fractions are $f_v = 0.119$ for $\kappa = 0$ and $f_v = 0.052$ for $\kappa = 2\epsilon$. This implies that the noncavitated portions of the samples have expanded far more in the tightly entangled systems, as might be expected from their larger $|P|$ (Figures 1b and 2b). The $\kappa = 0$ glass has a single large void oriented along the direction of extension, while the $\kappa = 2\epsilon$ glass has many (220) voids with a wide range of sizes and orientations. Small voids in this glass are—roughly speaking—homogeneously distributed throughout its volume, and many are quite far from the largest voids. The suppression of void growth in the more strain-localized lower half of this tightly entangled system, which necessarily leads to a more negative pressure, has clearly led to nucleation of many new voids in the "bulk" upper half. This is probably related to the recent observation that voids nucleate ahead of craze fronts in glasses approaching their fracture strains,[44,45] but verification would require larger system sizes that are beyond the capabilities of our current computational resources.

At the most qualitative level, all the κ-dependencies shown in Figures 2 and 3 are consistent with the traditional understanding of the crazing-versus-shearing competition.[28−30] Growth of voids along the axial direction requires the surrounding polymer to extend more rapidly than the surrounding bulk glass. Strong strain hardening suppresses this process because local axial tensile stresses are not large enough to produce such extension, especially in regions that have just cavitated. On the other hand, the fact that stronger strain hardening leads to larger $|P|$ and thus cannot suppress void *nucleation* has rarely been discussed, and to the best of our knowledge, the magnitude of these effects has not been previously reported.

4. DISCUSSION AND CONCLUSIONS

Recent advances in experimental techniques[44−47] have made it possible to study cavitation, void growth, and coalescence at a level of detail far beyond that achievable via traditional methods.[1,2] For example, Charvet et al. and Djukic et al. used[44,45] a combination of video-controlled tensile testing, surface tension measurements, scanning tunneling electron microscopy, and ultrasmall-angle X-ray scattering to compare deformation damage in cellulose acetate, PC, PMMA, and three polyphthalamide (PPA) glasses. They found that a significant number of crazes nucleate in ductile polymer glasses prior to yielding and then enter a stable-growth phase, wherein their growth rate is linear in the applied stress σ_{app}. At large strains, in moderately ductile glasses like PC and PMMA (but not extremely ductile ones like PPA), a subset of these crazes that grows faster (i.e. supralinearly) with σ_{app} appears; growth of this family leads to crack propagation and fracture. Here, we found that over the range $0.125 \lesssim \nu \lesssim 0.45$, our tightly entangled glasses more effectively suppress void growth. Specifically, they have not only significantly lower f_v (as expected[1,2]) but also significantly lower $d[\ln(f_{mv})]/d\epsilon$ while strain-hardening, for engineering strains up to 100%.

Another recently discovered, critical distinction between moderately and extremely ductile glasses is that in the former (but not the latter), new voids homogeneously nucleate just ahead of craze fronts, where $|P|$ is the highest.[44,45] These results were obtained from uniaxial-stress extension experiments, in which one cannot vary the strain and volumetric expansion ratio independently. We observed very little void nucleation in our uniaxial-stress extension runs, but our constant-ν results suggest that tighter entanglement promotes such homoge-

https://doi.org/10.1021/acs.macromol.1c01128
Macromolecules 2021, 54, 7347−7353

neous nucleation because it leads to larger |P| for a wide range of deformation histories. Experiments that combine techniques like those used in refs 44−47 with methods that offer precise control over the triaxial-stress state, e.g., tension-torsion experiments like those of Argon and Hanoosh,[48] might be especially fruitful.

Our main result—that tightly entangled glasses form far smaller (but far more) cavities than their loosely entangled counterparts at the same volumetric expansion ratio, for a wide range of ν—has not been previously reported. Previous simulations of the mechanics of glassy polymers deformed to large tensile strains missed this key feature because they (to the best of our knowledge) all employed either uniaxial-deformation (e.g. refs 7−16) or uniaxial-stress extension (e.g. refs 23−26). Needless to say, the complex mechanical histories experienced by glassy-polymeric samples in both experiments and real-world applications often follow neither of these protocols.

Promoting cavitation that does not lead to massive void growth and coalescence is clearly one of the keys to developing novel tough polymeric materials for high-performance applications. Our results suggest that one potential strategy is to engineer tightly entangled glass-forming polymers that retain a high level of elastic heterogeneity even when well-aged. Many of the chain stiffness-dependent differences reported herein may be understood in terms of the corresponding differences in segmental packing.[49] Our flexible-chain systems pack more efficiently; their initial density is $\rho_0 = 1.092$ in contrast to that of semiflexible chains' $\rho_0 = 1.073$. They also pack more homogeneously; the initial dispersion of their Voronoi volumes (calculated using voro++[50]) is $\Delta V_{voro}/\langle V_{voro}\rangle = 0.0374$, in constrast to semiflexible chains' initial $\Delta V_{voro}/\langle V_{voro}\rangle = 0.0423$. Cavitation is known to occur preferentially in regions with lower bulk moduli,[12] and the greater heterogeneity of our semiflexible glasses suggests that they have more such regions. It would be interesting to follow up our study by examining how the evolution of the elastic heterogeneity of these systems with increasing strain depends on κ and ν, using methods like those employed in refs 12 and 21.

We emphasize that here we have studied the athermal, $T \to 0$ limit where cavitation is stress-activated rather than being thermally activated and occurs only when the local energy barriers to void formation vanish. Increasing T will both lower these barriers (e.g., systems at higher T have lower ρ_0 and lower cohesive energy density) and allow thermal activation over them. Extending our studies by increasing T should allow systematic exploration of the resulting effects, which should improve our understanding of the $T \simeq T_{room} \simeq 3T_g/4$ regime where most real-world polymeric materials are applied.

Another remaining open question is: exactly what role do entanglements play in suppressing void growth? Simulations have shown that stable craze drawing (with concomitant void growth) in uncrosslinked glasses can occur with minimal entanglement loss and chain scission because entangled chain segments are free to move laterally over distances comparable to their rheological tube diameter.[15] This suggests that entanglements do not, by themselves, significantly suppress void growth until the dramatic hardening regime[9,37] immediately preceding craze breakdown and brittle failure is reached. Recent experimental results combined with mechanistic arguments[44,45] also suggest that the proximate cause of void growth suppression during ductile deformation is strain hardening rather than entanglement. On the other hand, unentangled glasses are very brittle, and $G_R \propto \rho_e$ (where ρ_e is entanglement density),[51] which makes isolating the role of entanglements challenging. One potential strategy for doing so is comparing $f_v(\epsilon, \nu)$ in glasses with the same G_R and flow stress σ_{flow}, but different ρ_e, over a wide range of ν.

AUTHOR INFORMATION

Corresponding Author

Robert S. Hoy − *Department of Physics, University of South Florida, Tampa, Florida 33620, United States;* orcid.org/0000-0003-0283-8117; Email: rshoy@usf.edu

Authors

Kai Nan − *Department of Physics, University of South Florida, Tampa, Florida 33620, United States*

Pedro Abritta − *Department of Physics, University of South Florida, Tampa, Florida 33620, United States*

Complete contact information is available at: https://pubs.acs.org/10.1021/acs.macromol.1c01128

Notes

The authors declare no competing financial interest.

ACKNOWLEDGMENTS

This study is based upon work supported by the National Science Foundation under grant no. DMR-1555242.

REFERENCES

(1) Kramer, E. J. Microscopic and molecular fundamentals of crazing. *Adv. Polym. Sci.* **1983**, *52*−*53*, 1.

(2) Kramer, E. J.; Berger, L. L. Fundamental Processes of Craze Growth and Fracture. *Adv. Polym. Sci.* **1990**, *91*−*92*, 1−68.

(3) Argon, A. S.; Cohen, R. E. Toughenability of polymers. *Polymer* **2003**, *44*, 6013−6032.

(4) Raghava, R.; Caddell, R. M.; Yeh, G. S. Y. The macroscopic yield behaviour of polymers. *J. Mater. Sci.* **1973**, *8*, 225.

(5) Rottler, J.; Robbins, M. O. Yield conditions for deformation of amorphous polymer glasses. *Phys. Rev. E* **2001**, *64*, 051801.

(6) Barney, C. W.; et al. Cavitation in Soft Matter. *Proc. Natl. Acad. Sci. U.S.A.* **2020**, *117*, 9157.

(7) Baljon, A. R. C.; Robbins, M. O. Simulations of Crazing in Polymer Glasses: Effect of Chain Length and Surface Tension. *Macromolecules* **2001**, *34*, 4200−4209.

(8) Rottler, J.; Barsky, S.; Robbins, M. O. Cracks and Crazes: On calculating the macroscopic fracture energy of glassy polymers from molecular simulations. *Phys. Rev. Lett.* **2002**, *89*, 148304.

(9) Rottler, J.; Robbins, M. O. Growth, microstructure, and failure of crazes in glassy polymers. *Phys. Rev. E* **2003**, *68*, 011801.

(10) Leonforte, F. Evolution of entanglements during the response to a uniaxial deformation of lamellar triblock copolymers and polymer glasses. *Phys. Rev. E* **2010**, *82*, 041802.

(11) Mahajan, D. K.; Singh, B.; Basu, S. Void nucleation and disentanglement in glassy amorphous polymers. *Phys. Rev. E* **2010**, *82*, 011803.

(12) Makke, A.; Perez, M.; Rottler, J.; Lame, O.; Barrat, J.-L. Predictors of Cavitation in Glassy Polymers under Tensile Strain: A Coarse-Grained Molecular Dynamics Investigation. *Macromol. Theory Simul.* **2011**, *20*, 826.

(13) Toepperwein, G. N.; de Pablo, J. J. Cavitation and Crazing in Rod-Containing Nanocomposites. *Macromolecules* **2011**, *44*, 5498.

(14) Venkatesan, S.; Basu, S. Investigations into crazing in glassy amorphous polymers through molecular dynamics simulations. *J. Mech. Phys. Solid* **2015**, *77*, 123.

(15) Ge, T.; Tzoumanekas, C.; Anogiannakis, S. D.; Hoy, R. S.; Robbins, M. O. Entanglements in Glassy Polymer Crazing: Cross-Links or Tubes? *Macromolecules* **2017**, *50*, 459.

(16) Ichinomiya, T.; Obayashi, I.; Hiraoka, Y. Persistent homology analysis of craze formation. *Phys. Rev. E* **2017**, *95*, 012504.
(17) Rottler, J.; Robbins, M. O. Shear yielding of amorphous polymer glasses: effect of temperature and strain rate. *Phys. Rev. E* **2003**, *68*, 011507.
(18) Riggleman, R. A.; Lee, H.-N.; Ediger, M. D.; de Pablo, J. J. Free volume and finite-size effects in a polymer glass under stress. *Phys. Rev. Lett.* **2007**, *99*, 215501.
(19) Hoy, R. S.; Robbins, M. O. Strain hardening in polymer glasses: Limitations of network models. *Phys. Rev. Lett.* **2007**, *99*, 117801.
(20) Hoy, R. S.; Robbins, M. O. Strain hardening of polymer glasses: Entanglements, energetics, and plasticity. *Phys. Rev. E* **2008**, *77*, 031801.
(21) Riggleman, R. A.; Lee, H.-N.; Ediger, M. D.; de Pablo, J. J. Heterogeneous dynamics during deformation of a polymer glass. *Soft Matter* **2010**, *6*, 287.
(22) Nguyen, H. T.; Hoy, R. S. Effect of the ratio l_K/p on glassy-polymeric shear deformation mechanisms. *Macromolecules* **2018**, *51*, 4370.
(23) Lyulin, A. V.; Balabaev, N. K.; Mazo, M. A.; Michels, M. A. J. Molecular dynamics simulation of uniaxial deformation of glassy amorphous atactic polystyrene. *Macromolecules* **2004**, *37*, 8785.
(24) Lyulin, A. V.; Vorselaars, B.; Mazo, M. A.; Balabaev, N. K.; Michels, M. A. J. Strain softening and hardening of amorphous polymers: Atomistic simulation of bulk mechanics and local dynamics. *Europhys. Lett.* **2005**, *71*, 618.
(25) Vorselaars, B.; Lyulin, A. V.; Michels, M. A. J. Deforming glassy polystyrene: Influence of pressure, thermal history, and deformation mode on yielding and hardening. *J. Chem. Phys.* **2009**, *130*, 074905.
(26) Vorselaars, B.; Lyulin, A. V.; Michels, M. A. J. Microscopic Mechanisms of Strain Hardening in Glassy Polymers. *Macromolecules* **2009**, *42*, 5829.
(27) Berger, L. L.; Kramer, E. J. The effect of temperature on the transition from crazing to shear deformation in crosslinked polystyrene. *J. Mater. Sci.* **1988**, *23*, 3536.
(28) Donald, A. M.; Kramer, E. J. The competition between shear deformation and crazing in glassy polymers. *J. Mater. Sci.* **1982**, *17*, 1871.
(29) Henkee, C. S.; Kramer, E. J. Crazing and shear deformation in crosslinked polystyrene. *J. Polym. Sci., Polym. Phys. Ed* **1984**, *22*, 721−737.
(30) *The Physics of Glassy Polymers*, 2nd ed; Haward, R. N., Young, R. J., Eds.; Chapman and Hall: London, 1997.
(31) Kremer, K.; Grest, G. S. Dynamics of entangled linear polymer melts - a molecular dynamics simulation. *J. Chem. Phys.* **1990**, *92*, 5057.
(32) Stevens, M. J. Interfacial Fracture between Highly Cross-Linked Polymer Networks and a Solid Surface: Effect of Interfacial Bond Density. *Macromolecules* **2001**, *34*, 2710−2718.
(33) *Polymer Glasses*; Roth, C. B., Ed.; CRC Press, 2016.
(34) Rottler, J. Fracture in glassy polymers: a molecular modeling perspective. *J. Phys.: Condens. Matter* **2009**, *21*, 463101.
(35) Everaers, R.; Sukumaran, S. K.; Grest, G. S.; Svaneborg, C.; Sivasubramanian, A.; Kremer, K. Rheology and microscopic topology of entangled polymeric liquids. *Science* **2004**, *303*, 823.
(36) Arruda, E. M.; Boyce, M. C. Evolution of plastic anisotropy in amorphous polymers during finite straining. *Int. J. Plast.* **1993**, *9*, 697.
(37) Hoy, R. S. Why is understanding glassy polymer mechanics so difficult? *J. Polym. Sci., Part B: Polym. Phys.* **2011**, *49*, 979.
(38) Plimpton, S. Fast parallel algorithms for short-range molecular dynamics. *J. Comp. Physiol.* **1995**, *117*, 1.
(39) Temperature is kept below $10^{-3}\ \epsilon/k_B$ during deformation runs using a Langevin thermostat with damping time $\tau_{Lang} = 10\tau$.
(40) Hopcroft, J.; Tarjan, R. Algorithm 447: efficient algorithms for graph manipulation. *Commun. ACM* **1973**, *16*, 372.
(41) Haward, R. N. Strain-hardening of thermoplastics. *Macromolecules* **1993**, *26*, 5860.
(42) Results for $\nu = .0625$ (not shown in the figures) are intermediate between those for $\nu = 0$ and $\nu = 0.125$.
(43) Meijer, H. E. H.; Govaert, L. E. Mechanical performance of polymer systems: The relation between structure and properties. *Prog. Polym. Sci.* **2005**, *30*, 915.
(44) Charvet, A.; Vergelati, C.; Sotta, P.; Long, D. R. Damage Mechanisms of Plasticized Cellulose Acetate under Tensile Deformation Studied by Ultrasmall-Angle X-ray Scattering. *Macromolecules* **2019**, *52*, 6613.
(45) Djukic, S.; Bocahut, A.; Bikard, J.; Long, D. R. Study of Damage Mechanisms of Amorphous and Low Semicrystalline Polymers under Tensile Deformation by Ultrasmall-Angle X-ray Scattering. *Macromolecules* **2020**, *53*, 5538.
(46) Bay, R. K.; Shimomura, S.; Liu, Y.; Ilton, M.; Crosby, A. J. Confinement effect on strain localizations in glassy polymer films. *Macromolecules* **2018**, *51*, 3647.
(47) Tiwari, S.; et al. Seeded laser-induced cavitation for studying high-strain-rate irreversible deformation of soft materials. *Soft Matter* **2020**, *16*, 9006.
(48) Argon, A. S.; Hannoosh, J. G. Initiation of crazes in polystyrene. *Phil. Mag.* **1977**, *36*, 1195−1216.
(49) Kumar, R.; Goswami, M.; Sumpter, B. G.; Novikov, V. N.; Sokolov, A. P. Effects of backbone rigidity on the local structure and dynamics in polymer melts and glasses. *Phys. Chem. Chem. Phys.* **2013**, *15*, 4604.
(50) http://math.lbl.gov/voro++/ (accessed in Oct. 2017).
(51) van Melick, H. G. H.; Govaert, L. E.; Meijer, H. E. H. On the origin of strain hardening in glassy polymers. *Polymer* **2003**, *44*, 2493.

https://doi.org/10.1021/acs.macromol.1c01128
Macromolecules 2021, 54, 7347−7353